

RESEARCH ON THE AERODYNAMICS OF BLADE PROFILES OF WIND TURBINES

POP E. S., CAMPEAN E., DRAGAN T.

Technical University of Cluj-Napoca, Memorandumului no.28, Cluj-Napoca,
emanuelapop13@gmail.com

Abstract –Small capacity wind turbine performance is influenced in a large extent by the blade profiles aerodynamics. By this point of view, the paper presents the most important aspects of aerodynamic profiles, and aspects concerning their optimization in order to increase performance. The study of blade profiles polar led to the identification of a reference profile, NACA4418, for which the best aerodynamic lift drag ratio is obtained on a big range of attack angles. A flow analysis on the reference profile is performed, using a CFD model of numerical simulations in order to obtain performance for different wind speeds.

Keywords: airfoil profile, renewable energy, aerodynamic performance, drag, lift, CFD.

1. INTRODUCTION

Aerodynamics is a science derived from fluid mechanics, studying the effects due to the relative motion of incompressible fluids and solids, and the effects caused by the motion of bodies in the air. The usual fluids are air, water, gas and out of the best known applications we mention the study of gas flow through pipelines, wind effects on buildings and numerous applications in aeronautics. In the case of wind turbines, the aerodynamic principles are found in the form of blades and their functioning, specifically at the air flow around the blades.

The laws that govern the principles of aerodynamics and explain the phenomena that takes place at the air interaction with solids are the law of conservation of mass, continuity equation and Bernoulli's law.

Lift phenomenon is explained by the fundamental law of flow or Bernoulli's Law, which expresses that the sum of kinetic and potential energies of fluid mass remains constant in any section of the drain tube if there is no energy loss. The amount of static pressure, dynamic and the hydrostatic pressure is a constant (called total pressure) for each section. The law is expressed by Bernoulli's equation [1, 2] by the following relation (1).

$$p_1 + \rho \frac{u_1^2}{2} + \rho gh_1 = p_2 + \rho \frac{u_2^2}{2} + \rho gh_2 \quad (1)$$

where p is the static pressure, $\rho \frac{u^2}{2}$ is the dynamic pressure, ρgh is the hydrostatic pressure, ρ is the fluid

density (in the considered air case), U is the flow velocity of the fluid, and h is the height from the position regarded as the reference.

In the case of the wind turbine the height is considered constant, thus simplifying the hydrostatic pressure and the equation becomes:

$$p_1 + \rho \frac{u_1^2}{2} = p_2 + \rho \frac{u_2^2}{2} \quad (2)$$

The sum of the static and dynamic pressure is constant, thus with the increase of the dynamic pressure the air flow speed around the blade decreases as the static pressure decreases. Dynamic pressure occurs in the direction of flow and static pressures are manifested with equal intensity in all directions. Thus, to a fluid flowing with speed the pressure increase will occur in the direction of the flow, due to the dynamic pressure component as well as the pressure drop in the perpendicular direction to the flow.

Wind turbine blades are the most popular aerodynamic profiles obtained by sectioning them horizontally, in case of vertical axis turbines, or vertically, for turbines with horizontal axis. They are responsible in a large extent for the performance and the aerodynamic characteristics of the wind turbine [3].

2. AERODYNAMIC PROFILE PARAMETERS

2.1 Geometric parameters for aerodynamic profiles

The main parameters that define the aerodynamic profiles are shown in Figure 1:

- c profile chord connecting the extreme points of the profile, A and B ;
- leading edge, A , is the highest point on the front of the profile, which strikes the air mass;
- trailing edge, B , is the farthest place through which air masses leave the profile;
- the **extrados** is the outer surface of the profile between the leading edge and trailing edge;
- the **intrados** is the underside of the profile between the leading edge and trailing edge;
- the **center line** of the profile unites the leading edge and trailing edge and any point on this line is equally distant of intrados and extrados;
- the maximum curve C_{max} , is the maximum distance between the center line and the chord;

- the location of maximum curvature x_{Cmax} ;
- the maximum thickness of the profile G_{max} ;
- the maximum thickness position x_{Gmax} .

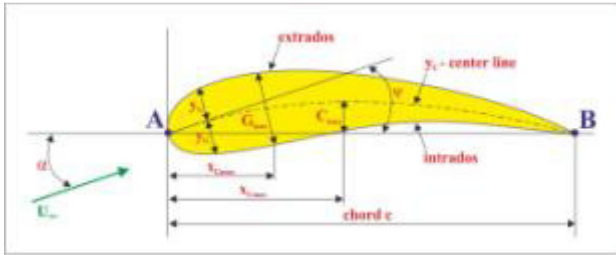


Fig. 1. Geometric parameters for aerodynamic profiles

Thus, for the NACA 4418 blade profile we can say that the maximum curve is 4%, situated at 40% of the chord with a thickness of 18%, while for the profile NACA 0018, which is a symmetric profile, the maximum curve is 0%, so the default maximum curvature and location, and the maximum thickness is 18%. Percentages are calculated corresponding to chord length. The coordinates are obtained by combining the coordinates of the mean curvature line and thickness distribution.

2.2 The attack angle

The angle between the airflow directions with the profile chord is called angle of incidence or angle of attack, and it can be (Figure 2):

- positive, the angle between the profile chord and the direction of airflow on the intrados;
- negative, the angle between the profile chord and the direction of airflow on the extrados;
- null, when the air flow strikes the front of the profile and the movement corresponds to the profile chord direction.

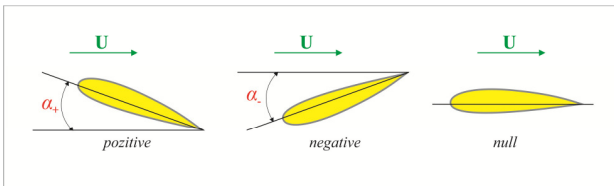


Fig. 2. Angle of attack

Over the years there have been various studies on the blade profiles, many of these are for the achievement of high capacity turbines. These profiles were grouped in different families and can be found in various catalogs of the industry.

The most common profiles are Eppler (E 168, E178), Wortmann (FX60-126-1, FX63-137, FX77-W-153, FX77-W-258), NACA, class N (N60, N60R), RAE, Gottingen (GOE358, GOE176, GOE496), NLR, NASA, SANDIA and Berghey WindPower (SH3052, SH3055, BW-3), NREL (S1210, S822, S834) [1, 4].

NACA (National Advisory Committee for Aeronautics) is the most popular and complex family of blade profiles among multiple applications in wind turbines, and also in the case of numerical validations, with different grades depending on the type of turbine.

2.3 Forces on an aerodynamic profile

Betz's theory indicates the ideal value for the extraction of the mechanical energy from an air current without considering the power converter shape. However, in the real world, the power that can be retrieved is independent of its characteristics. The fundamental difference lies in the type of the aerodynamic force that is used to produce mechanical energy. The aerodynamic forces acting on the profiles consist of the drag force, in the direction of flow and lift, and the aerodynamic lift force, which is perpendicular to the direction of flow (Figure 3). The rotation of the blades is due to the lift force, therefore optimizing the aerodynamic profiles aims to get a bigger lift force [5,6,7].

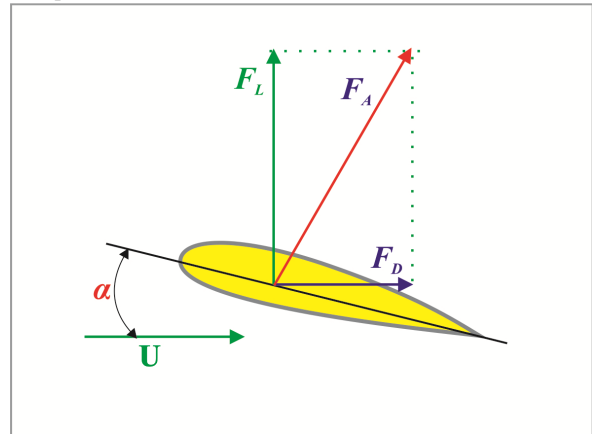


Fig. 3. Forces acting on an aerodynamic profile

The air stream moves in the direction AB and when it meets the aerodynamic profile it is distributed on the two surfaces of the profile. Air particles leaving at the same time the leading edge of the profile, due to the law of conservation of mass, are simultaneously reaching to the trailing edge (Figure 4).

The road traveled by the air particles is greater on the upper side than on the lower, due to the shape of the profile, so the flow rate is higher on the extrados and, according to Bernoulli's law, the static pressure is lower than on the intrados [8,9,10]. The lift force appears due to this difference of pressure on the profile and it is proportional to the pressure difference on the two surfaces of the profile. Depending on the positioning of the profile in the air flow, the lift force may be higher [2].

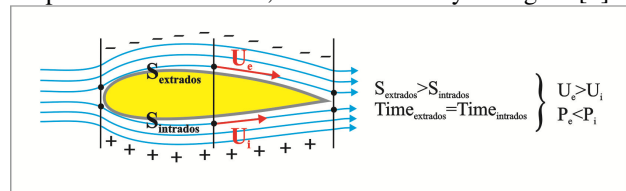


Fig. 4. The appearance of the lift force

The total aerodynamic force, F_A , acting on a body moving in an air stream, is the air resistance opposed by the movement of the body [2, 4, 15].

$$F_A = \frac{\rho U^2}{2} \cdot A_p \cdot C_A \tag{3}$$

The force parallel to the direction of the flow called drag force is calculated by the equation (4), and the force perpendicular to the direction of flow, that is the lift force, is obtained by the equation (5).

$$F_D = \frac{\rho U^2}{2} \cdot A_p \cdot C_D \quad (4)$$

$$F_L = \frac{\rho U^2}{2} \cdot A_p \cdot C_L \quad (5)$$

The total aerodynamic force is obtained from the composition of drag force and lift force [2, 4, 15].

$$F_A^2 = F_D^2 + F_L^2 \quad (6)$$

$$F_A = \sqrt{F_D^2 + F_L^2} \quad (7)$$

where: ρ is density of air, U the current velocity in m/s, A_p the profile area profile in m^2 , C_A is a dimensionless coefficient that depends on the shape, surface condition and the angle of incidence of the body called the coefficient of the total aerodynamic force, C_L is the dimensionless coefficient of lift, and C_D is the dimensionless drag coefficient.

Following the theoretical and experimental studies in the wind tunnel depending on the angle of attack, the pressure distribution on the aerodynamic profile and the appearance of aerodynamic forces were outlined. Thus, for null angles on the intrados and extrados of the profile, depressions will be formed, which cancel each other, so the lift force is void, while on the profile will act only the drag force (Figure 5a).

At positive angles of attack, small (Figure 5b) and normal (Figure 5c) depressions will be formed on the extrados and pressures on the intrados, which summed up give the lift force, which will be growing with increasing depressions on extrados.

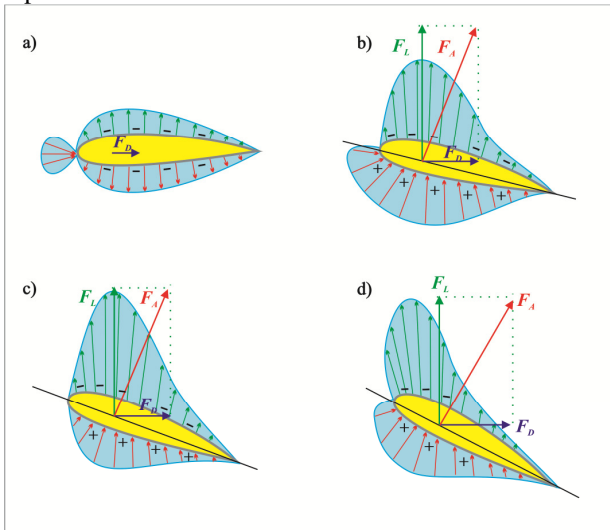


Fig. 5. Profile pressures repartition

Near the critical angle, the depressions area on the extrados moves to the leading edge, and the pressure increases, in this area the lift force reaches the maximum capacity (Figure 5d). After exceeding the critical angle, the lift force decreases and the drag force increases.

Forces acting on an aerodynamic profile have their origin in the same point. This is called the center of pressure point and its position varies according to the angle of attack, due to changes in position of the depression and pressure areas from the upper surface or the underside of the profile. Therefore, for angles of 20° and 15° , the center of pressure is closer to the leading edge, while for an angle between 15° and 0° it departs.

3. AERODYNAMIC PROFILE POLARS

Aerodynamic profiles are influenced considerably and behave differently depending on the Reynolds number. While for large capacity turbines, the corresponding Re numbers are greater than 1,000,000 [11], for small capacity turbines they are between 100,000 and 500,000 [4].

Reynolds number value for different profiles is obtained by the relationship:

$$Re = \frac{\rho U l}{\mu} = \frac{U l}{\nu} \approx 71 U l \quad (8)$$

where ν is the kinematic viscosity coefficient, U is the characteristic speed and l is the characteristic length, which in case of blade profiles is equal to the length of the chord.

Depending on the size of the Re number, the airflow may be turbulent or laminar.

The performance of the aerodynamic profiles is determined and the moment C_m coefficient, defined by the following relationships [11, 4, 15]:

$$C_D = \frac{F_D}{\frac{1}{2} \rho U_{rel}^2 A_p} \quad (9)$$

$$C_L = \frac{F_L}{\frac{1}{2} \rho U_{rel}^2 A_p} \quad (10)$$

where ρ is the air density, U_{rel} is the relative speed of airflow in m/s, A_p is the profile area in m^2 , F_L is the lift force and F_D is the drag force.

Polar curve specific to a certain aerodynamic profile is shown in Figure 6. $C_L(\alpha)$ curve varies linearly in the field of small attack angles, positive and negative, and as we approach the critical angle of attack value, the curve is modified and will have smaller values, due to the detachment phenomena of air fillets on the profile before employment. $C_L(\alpha)$ curve intersects the Ox axis at a α value called null lift angle and Oy axis at an angle of attack $\alpha = 0$. Overall null lift angle is between -2° and -6° . In the case of symmetrical profiles, the $C_L(\alpha)$ curve passes through the origin.

$C_D(\alpha)$ curve is a parabolic curve, with linear variation areas, that intersect the axis of ordinates at an angle of attack $\alpha = 0$.

In order to understand the dependence of the aerodynamic coefficients, we proposed for analysis the $C_L(C_D)$ curve obtained throughout the Profil software, version 2.30 (Figure 7).

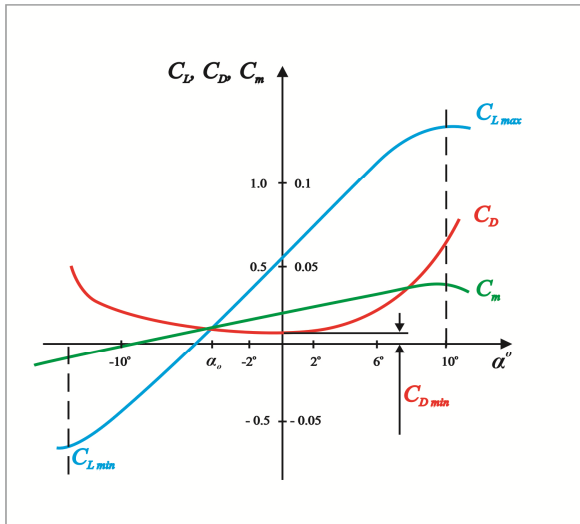


Fig. 6. Profile polar

The angle of attack is 0 in point 1 as it is represented in the figure. At this point, the value of the lift force is zero. By drawing the perpendicular to Ox axis, that is tangent to the curve, point 2 is obtained in the tangent area and it corresponds to the minimum value of the drag force. The tangent to the curve passing through the origin intersects the curve in point 3, for which the angle θ is minim and the profile finesse C_L/C_D is maximum. The perpendicular to the Oy axis allows finding the maximum value of C_L in point of tangency to the curve 4.

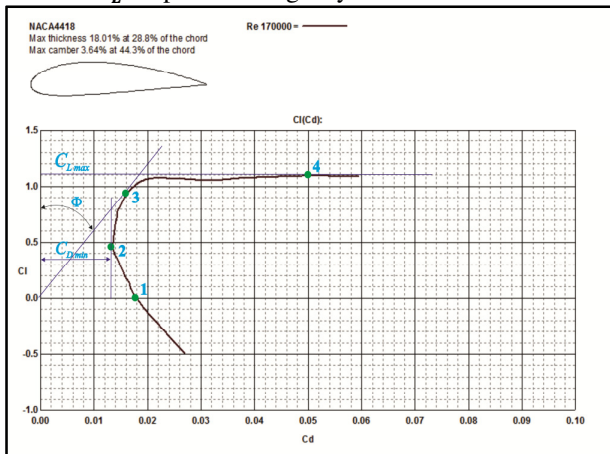


Fig. 7. Polar curve

Choosing the reference profiles

It is very important to choose a right profile for low-capacity wind turbines, as this directly affects their performance.

When choosing the type of blade for a wind turbine, one must take into account several aspects:

- there is a large variation of the Reynolds number on the blade length, which corresponds to the limit $Re \approx (0.1 \dots 0.5) \times 10^6$;
- resistance coefficient tending to zero;
- the increase of the lift coefficient and its expansion in the widest possible limit of the angle of attack α ;
- blade section must work properly, both the low incidence and the high incidence;
- the possibility to increase the profile thickness in order to obtain a resistant structure ;

- locating the wind turbine;
- the low cost of implementation and a good surface quality that it will contribute both to the increase of performance and to the reduction of vibration and noise.

The polar study was carried out for three different blade profiles of the NACA family: two symmetric profiles, NACA 0018 and 0015, and an asymmetric profile section, NACA 4418. Drawing the polar and analysis of these blade profiles was performed in version 2.30 of Profil software. With the help of the software, the following were carried out: the polar drawing for different Reynolds numbers, the comparison between a group of profiles and the analysis of the pressure distribution for each profile [12].

As noted previously, small capacity wind turbines operate at lower wind speeds, implicitly at low Reynolds numbers, thus for the analysis, their field ranges between 80,000 and 500,000. To this area it corresponds a wind speed that ranges between 5 m/s and 37 m/s, being a rank of speeds between the starting speed (CIS) and the cut out speed (COS) of the turbines.

The results for each blade profile, at different values of Re, is presented in [12] and in Figures 8 and 9 are compared the aerodynamic coefficients for NACA 0015, NACA 0018 and NACA 4418 profiles, for the number Re equal to 170,000 and 300,000, that is for wind speeds of 12-13 m/s and 22 m/s.

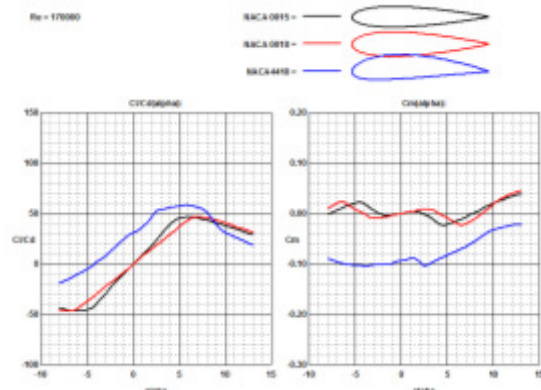


Fig. 8. Comparison of the aerodynamic coefficients for NACA 0015, NACA 0018 and NACA 4418 profiles for Re=170000 (Profili v2.30a).

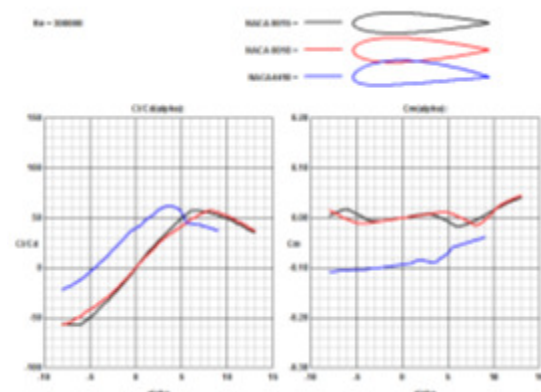


Fig. 9. Comparison of the aerodynamic coefficients for NACA 0015, NACA 0018 and NACA 4418 profiles for Re=300000 (Profili v2.30a).

NACA 4418 profile has the best performance for which the profile finesse C_L/C_D is higher almost on the entire field, so it is justified its choice as the reference model for the rest of the simulations.

4. THE NUMERICAL SIMULATIONS

The mathematical modeling of flow process, over the reference profile was carried out in Ansys software, Fluent solver. For this, it has been used the CFD numerical simulation models (Computational Fluid Dynamics) and the finite volume method, because this method allows modeling and simulating laminar and turbulent flow, heat transfer, chemical reactions and other phenomena of interest.

In order to best capture the flow around profiles it is important to set a fine grid. Thus, a boundary layer of 15 layers was carried out, with a growth factor of 1.15, finally resulting in a grid of 22 million tetrahedral elements. Details of the meshing grid can be seen in Figures 10 and 11, around the profile, as well as details of the blade front end and back end.

Due to the stationary flow regime, a stationary work with a solver based on pressure was selected. The fluid that was elected is an incompressible gas with properties similar to the air, and the turbulence model used was SST $k-\omega$. Details regarding the choices for setting up the case and other important aspects in order to achieve these simulations are represented in [13,14].

To get relevant results, as close to the real environment as possible, the choice for specific speeds was made for different values of undisturbed wind, between 2.5 m/s and 20 m/s. Consistent with urban or rural operating environment of the small capacity wind turbines, the reference values for wind chosen for illustration are 5 m/s, 10 m/s and 15 m/s with the corresponding specific speed of 5.02, 2.51 or 1.67.

The pressure coefficients fields on the reference profile surface for the three specific speed values are



Fig. 12. The pressure coefficients field for NACA 4418 profile for specific speeds: a. $\lambda=5.02$; b. $\lambda=2.51$; c. $\lambda=1.67$.

Axial velocity fields (Figure 13) and vectorial velocity fields (Figure 14) show the influence of blade profile relative to the wind speed, and the phenomena that occurs from the interaction with it. Thus, due to friction between the profile and the airflow, the velocity in the boundary layer is lower, as well as the type of flow on the upper surface and underside of the profile relative

represented in Figure 12. In small capacity turbines operating at low values of Re numbers, the optimum values for the angle of attack, for which the profile gets the best aerodynamic finesse, C_L/C_D , are between 4° and 7° . The reference blade profile is located in the airflow in an optimal position for the angle of attack equal to 5° .

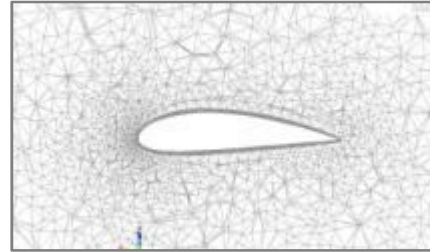


Fig. 10. Detail of the meshing grid for NACA 4418 profile

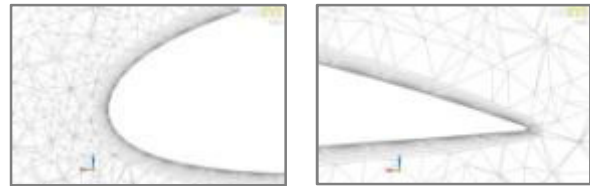


Fig. 11. Detail of the meshing grid for NACA 4418 profile, in front end and back end

According to figures, it can be seen that with increasing velocity, by default the lift force, on the extrados of the profile there is an increase of depressions, while on the intrados there is a decrease of pressures. The conducted simulations have revealed that with increasing wind speed the static pressure decreases, which acts in the perpendicular direction to the flow direction and the pressure coefficient, resulting an increase of the lift force and of the power coefficient generated by the turbine.

speed on the extrados of the profile. Laminar flow area increases with speed, while the turbulent flow decreases with it.

Turbulence intensity fields are represented in Figure 15 and, as in the case of speed fields, with the increase in

wind speed, the turbulence area is decreasing. Turbulences are characterized as being chaotic, and they fluctuate in all directions causing the formation of vortices of different scales, with adverse effects on the performance of wind turbines.

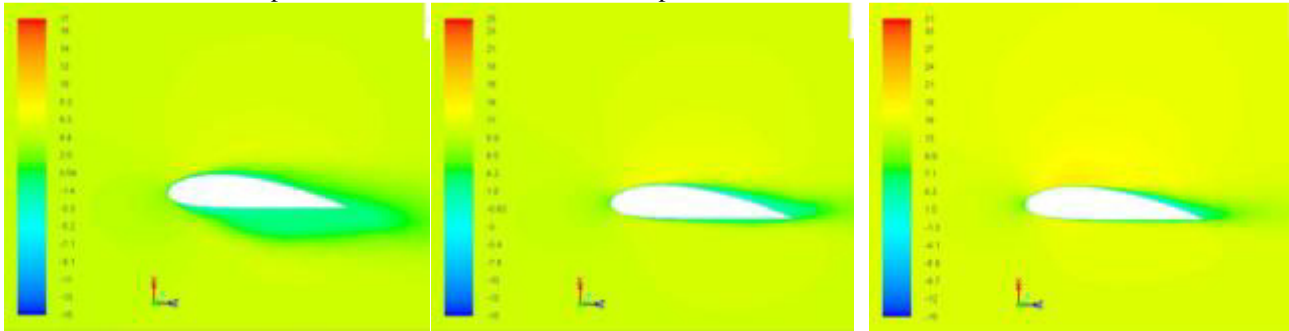


Fig. 13. The axial speed field for NACA 4418 profile at specific speeds: a. $\lambda=5.02$; b. $\lambda=2.51$; c. $\lambda=1.67$.

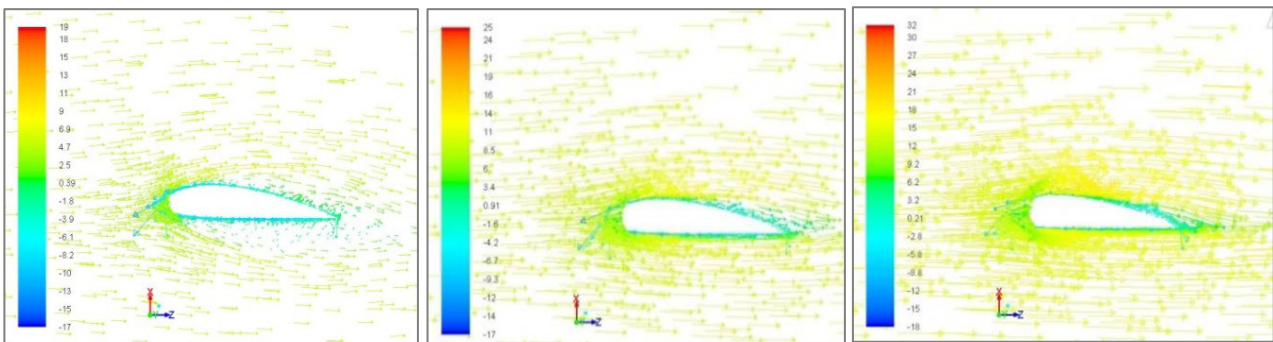


Fig. 14. The vectorial speed field for NACA 4418 profile at specific speeds: a. $\lambda=5.02$; b. $\lambda=2.51$; c. $\lambda=1.67$.

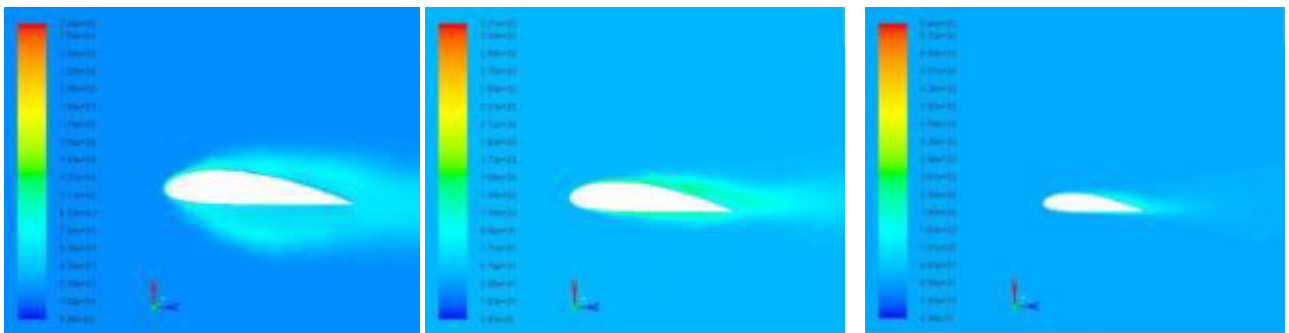


Fig. 15. The turbulence intensity fields for NACA 4418 profile at specific speeds: a. $\lambda=5.02$; b. $\lambda=2.51$; c. $\lambda=1.67$.

5. CONCLUSIONS

The profile polar analysis assisted the choice of the reference profiles and it also offered a number of issues regarding optimization. During the research, it was observed the influence of the angle of attack on the aerodynamic coefficients. Thus, it was observed that with the increase of the chamber, the aerodynamic coefficients increase as well, while the attack angle decreases. The drag coefficient C_D increases with relative thickness, and the C_L lift coefficient is maximum for profiles with relatively middle thickness. On the other hand, the lift coefficient increases C_L according to the Re number.

In particular, for vertical axis wind turbines, the selection of the angle of attack is essential, and so is finding variants in which the blade is in the optimal position, because the power coefficient variation is caused by the continuous change of the angle of attack with turbine blade rotation. To decrease this invariableness performance it is required for new constructive solutions to be found, that take into account all these aspects.

The aerodynamic profiles are responsible for a large proportion of wind turbine performances, especially when it comes to small capacity turbines operating in urban or rural environments, characterized by lower wind speeds and sudden changes of direction. For this reason, it is essential to choose an optimized

profile, so that the turbine can extract maximum energy and turn it into electricity.

Besides the importance of the aerodynamic profiles, an important role plays also the overall construction of the wind turbine, due to fluctuations in wind speed and direction. Currently, small capacity wind turbines have a power coefficient of about 0.25, compared to 0.45 of the high-capacity turbines.

REFERENCES

- [1]. Paraschivoiu, I. –Subsonic Aerodynamics, Polytechnic International Press, Canada, 2003, ISBN 2-553-01130-X.
- [2]. Popovici, D. – Principiile zborului. Aeroclubul României, 2003.
- [3]. Wolfe, W.P. and Ochis, S.S., – Predicting Aerodynamic Characteristics of Typical Wind Turbine Airfoils Using CFD, Sandia National Laboratories, Sandia Report, SAND96-2345, 1997.
- [4]. Ciupercă, R. – Contribuții la elaborarea și cercetarea rotorului eolian elicoidal, Teză de doctorat, Chișinău, 2010.
- [5]. Kurtulmus, F., Vardar, A. and Izli, N. – Aerodynamic Analysis of Different Wind Turbine Blade Profile, 2007.
- [6]. Abbott, I.H. – Theory of Wing Sections, 1959.
- [7]. Gundtoft, S. – Wind Turbines, Engineering College of Aarhus, 2008.
- [8]. Sheldahl, R.E., Klimas, P.C., Feltz, L.V. – Aerodynamic performance of a 5-metre-diameter Darrieus turbine with extruded aluminium NACA-0015 blades, 1980, <http://www.prod.sandia.gov/cgi-bin/techlib>.
- [9]. Sherwood, K. – Blade Manufacturing Improvement Project: Final Report, 2002, <http://www.sandia.gov:80/wind/other/030719.pdf>.
- [10]. Klimas, P.C. and Sheldahl, R.E. – Four Aerodynamic Prediction Schemes for Vertical-Axis Wind Turbines - A Compendium, SANDIA National Laboratories, SANDIA Report, 1978, SAND78-0014.
- [11]. Dumitrescu, H., Georgescu, A., et al. – Calcululei, Editura Academiei Române, Bucuresti, 1990, ISBN 973-27-0053-X.
- [12]. Souca (Pop), E. – Airfoil selection for aerodynamic performance criterion on small wind turbines, Acta Technica Napocensis, Cluj-Napoca, Vol. 57, Issue 2, 2014.
- [13]. Pop, E., Ciupan, C. – Mathematical modeling of flow processes for wind turbines, International Conference on Production Research- Africa, Europe and the Middle East – 4th International Conference on Quality and Innovation in Engineering and Management, Cluj-Napoca, 2016.
- [14]. Souca (Pop), E. – Cercetări și contribuții privind construcția turbinelor eoliene de putere mică”, Teză de doctorat, Cluj-Napoca, 2014.
- [15]. Paraschivoiu, I. – Wind Turbine Design: With emphasis on Darrieus Concept, Polytechnic International Press, Montreal, 2002.